2012

Alternative Heat Rejection Methods for Power Plants

R. A. Leffler
Purdue University

C. R. Bradshaw
Purdue University

E. A. Groll
Purdue University

S V. Garimella
Purdue University, sureshg@purdue.edu

Leffler, R. A.; Bradshaw, C. R.; Groll, E. A.; and Garimella, S V., "Alternative Heat Rejection Methods for Power Plants" (2012). *CTRC Research Publications.* Paper 159.
http://dx.doi.org/10.1016/j.apenergy.2011.10.023

Alternative Heat Rejection Methods for Power Plants*

Robert A. Leffler[a,b], Craig R. Bradshaw[a,b], Eckhard A. Groll[a,b], Suresh V. Garimella[b,**]

[a]*Herrick Laboratories, School of Mechanical Engineering, Purdue University, 140 S. Martin Jischke Drive West Lafayette, IN 47907-2031, USA*

[b]*Cooling Technologies Research Center, an NSF IUCRC, Purdue University, 585 Purdue Mall West Lafayette, IN 47907-2088, USA*

*Submitted for possible publication in *Applied Energy*, July 2011, and in revised form, September 2011

***Author to whom correspondence should be addressed: sureshg@purdue.edu*

Abstract

Process waste heat in large power generation plants is commonly rejected to lakes or rivers, or through the use of cooling towers. Although these waste heat rejection methods are effective, they may not be feasible in every application due to cost considerations or geographic location. Moreover, it is desirable to put some of the waste heat to good use, both from the standpoint of improved plant efficiency as well as reduced environmental impact. An analysis of alternative methods of power plant waste heat rejection is presented here as applied to a coal-fired power generation facility in the Midwestern United States. Five approaches for rejecting or recovering the waste heat are considered: cooling canals, open-water algae bioreactors, wintertime greenhouse heating, spray ponds, and modified solar updraft towers. Each of the five technologies can be sized for the needs and operating conditions of a given power plant. The quantitative analysis tools developed in this work are validated by benchmarking against published results. Three of the alternative methods generate secondary benefits: the algae bioreactor, greenhouse heating, and the modified solar updraft tower produce biodiesel, extended periods for horticulture, and electric power, respectively. The land area required to reject 1.16 GW of heat (the condenser heat rejection from a 500 MW plant operating at 30% thermal efficiency) using each of the alternative technologies is compared. The sensitivity of the sizing of the different technologies to changes in the environmental and geometric parameters is quantified. Finally, the net water use for each technology is estimated and compared against a typical cooling tower solution for the same 500 MW plant.

Keywords: Waste heat recovery; energy efficiency; power plant; cooling canal; algae bioreactor; greenhouse heating; spray ponds; updraft tower; water use

1. Introduction

Basic thermodynamic considerations result in the production of a large amount of waste heat in power plants. For each megawatt of electricity generated, approximately two megawatts is discharged in the form of waste heat. The most common methods of handling the waste heat in large power plants involve rejection to lakes and streams, or the use of cooling towers. These methods are well established, offer reliable operation, and provide a working fluid return temperature that is close to that of the environment. However, heat rejection into lakes and streams may result in an undesirable increase in water temperature that could alter the bio-equilibrium and have a significant impact on living organisms in these water bodies. On the other hand, heat rejection using cooling towers can be costly and consumes large amounts of water. Furthermore, both of these heat rejection options do not provide a means for recovering any of the rejected heat for useful purposes. It is important to explore and assess other options for heat rejection that may prove to be viable alternatives. The present work explores five such heat rejection options for large power plants, including a detailed analysis and comparison study. These methods include cooling canal systems, algae bioreactors, wintertime heating of greenhouses, spray ponds, and modified solar updraft towers.

A shallow-water canal system can be used to cool the condenser discharge water with atmospheric air before re-entry to the condenser or discharge to a lake. As in a cooling pond, heat is rejected from the canal through a combination of convection and radiation heat transfer as well as evaporation of canal water. Cooling canals can be used to reject a portion of the required heat, or as the sole source of heat rejection from the power plant. A cooling canal system near Turkey Point, Florida, was evaluated by Frediani [1], who showed that 4.7 GW of heat could be rejected from the system consisting of 32 outflowing canals and 7 return canals. Each canal is 8,380 m long and 90 m wide, for a total cooling canal area of 17.7×10^6 m^2.

An open-water algae bioreactor pond transfers heat from condenser discharge water to a shallow pond with a layer of algae growing on the surface. The algae bioreactor pond is designed to operate without the aquatic life typical of cooling reservoirs, and may be operated at elevated temperatures. Species of thermophilic algae are grown in the bioreactor pond, with the algal biomass collected at specified intervals and processed into a biofuel or other fuel source. Recent studies have shown that biofuels derived from algae have the potential to provide a renewable fuel with a lower life-cycle energy cost than petroleum fuels [2,3]. Ryan *et al*. [4] evaluated the surface heat loss from the Hazelwood cooling pond in Victoria, Australia, and from Lake Hefner in Oklahoma City, Oklahoma. A theoretical model was used to evaluate cooling due to wind-driven forced convection as well as natural convection, and served to demonstrate the use of cooling ponds for heat rejection as well as algal growth.

A greenhouse heated in the wintertime by the waste heat discharged from a power plant could produce agricultural products year-round in northern climates. Condenser discharge water pumped through pipes in the soil transfers heat to the greenhouse through conduction. Chinese *et al*. [5] designed a greenhouse heating system in Northeastern Italy heated by waste heat from a 2 MW plant fueled by scraps of wood from the chair-manufacturing industry. Manning and Mears [6] evaluated a greenhouse 11,000m^2 in area in Washingtonville, Pennsylvania, heated by condenser discharge water

from the PP and L Montour County Generating Station. In addition, Chou *et al.*[7] presented a simple analytical heat transfer model of a greenhouse space. These studies show that a greenhouse is a feasible method to exploit waste heat and can be modeled effectively.

A spray pond uses an array of water fountains issuing from the surface of a cooling pond. Heat is rejected from the spray droplets and the pond surface through evaporation of water and convection heat transfer. Previous works have modeled the heat transfer in such situations, and accounted for flow of the surrounding air. Analytical models have been developed by Chen and Trezek [8] and Porter and Chaturvedi [9], in which the thermal performance of the spray was expressed in terms of Number of Transfer Units (NTU). Spray ponds have been successfully used as the sole sources of heat rejection from nuclear power plants in a number of geographic locations around the United States [10].

A classic solar updraft tower consists of a large solar collector at the base of a tower and a gas turbine where the collector and tower meet. The solar updraft tower effectively captures solar energy through the greenhouse effect, and converts it into kinetic energy of atmospheric air through the suction of the tower which relies on a temperature differential along its length. Atmospheric air is drawn due to the suction of the tower into the solar collector at the base of the tower where it is heated before passing through the wind turbine and into the tower. Padki and Sherif [11] developed an analytical model for solar updraft towers. Their analytical model simplified the effects of various geometrical and operating parameters on tower performance. A similar model was recently extended to include a more detailed model of wind turbine pressure drop within a solar tower [12].With a modified solar updraft tower, heat is rejected from the power plant via a heat exchanger distributed around the perimeter of the solar collector at the base of the tower. The heat exchanger rejects heat from the power plant as it preheats the air going into the solar collector. The fluid in the heat exchanger tubes is a refrigerant in a secondary circuit between the condenser of the plant and the atmospheric air. The modified tower can operate merely with heat rejected from the power plant, and solar heating is not essential to its operation.

2. Analytical Modeling

Each of the alternative heat rejection options analyzed in this work targets a 500 MW power plant. Assuming the plant operates at 30% thermal efficiency (although higher efficiencies are common), the plant needs to reject 1.16 GW. This heat is assumed to be available in the form of a water stream flowing from a cooling condenser within the power generation plant. To maximize thermodynamic efficiency, power generation plants operate with the lowest condenser temperature as possible (as low as 35-40 °C for the most efficient plants). Therefore, for a typical 500 MW power plant the waste heat is assumed to be available at 45 °C. The alternative waste heat options considered are each assessed against this heat rejection requirement under humid, summer conditions. The ambient temperature is assumed to be 30°C, and the ambient pressure is taken as 101.325 kPa. The ambient relative humidity and wind speed are 70% and 4 m/s, respectively. These conditions represent a typical summer day in the Midwestern United States. These conditions are typical of the Midwestern United States and can

vary significantly across the country, particularly in the warmer and drier climates of the Southwestern United States. In addition to summer conditions, the greenhouse heat rejection option is also analyzed under a variety of winter conditions.

Each technology is also benchmarked for water use against the estimated amount for a typical cooling tower as a reference. A recent DOE study reports that a 500 MW coal-fired power plant uses roughly 7000 gpm (26.5 m^3/min) of makeup water during typical operation [13]. This is water that is lost to the environment during typical operation. This corresponds to roughly 441 kg/sec of water being lost to the environment.

2.1. Cooling Canal:

The cooling canals reject heat through a combination of convection and radiation heat transfer as well as evaporation of canal water. The performance of a single canal is analyzed by discretizing into increments along the flow path. The water in the canal is assumed to be well mixed from the surface to the bottom of the canal. Figure 1 illustrates the control volume at a single section of the canal. As a conservative approximation, the bottom of the canal is assumed to be insulated, that is, no heat is transferred to the ground at the bottom or the sides. The enthalpy change is calculated from the heat transferred in each segment:

$$\dot{m}_i \mathbf{h}_i - \dot{m}_{i+1} \mathbf{h}_{i+1} + \dot{Q}_{solar} = \dot{Q}_{evap} + \dot{Q}_{conv} \tag{1}$$

$$\dot{Q}_{solar} = A\left[\alpha_{solar} G_{rad} - \varepsilon\sigma\left(T_s^4 - T_{sky}^4\right)\right] \tag{2}$$

$$\dot{Q}_{conv} = hA\left(T_s - T_\infty\right) \tag{3}$$

$$\dot{Q}_{evap} = h_{hm}\left(\rho_{vapor,s} - \rho_{vapor,\infty}\right) h_{fg} A \tag{4}$$

in which the convection coefficient is given by Churchill and Ozoe [14] as,

$$h = \frac{\left(k_{air}/L\right) 0.6774 Pr^{1/3} Re_{crit}^{1/2}}{\left[1 + \left(0.0468/Pr\right)^{2/3}\right]^{1/4}} + 0.037 Pr^{1/3}\left(Re_L^{4/5} - Re_{crit}^{4/5}\right) \tag{5}$$

$$h_{hm} = \frac{h}{\rho_{air} c_p Le^{2/3}} \tag{6}$$

This calculation is performed for each segment, where the enthalpy exiting one segment becomes the enthalpy entering the next consecutive segment. Variations in solar radiation are accounted for by a solar influence factor, which represents the fraction of the maximum solar radiation absorbed by the canal. In this analysis, the solar influence factor is assumed to be 30% due to nighttime conditions and

average daytime cloud cover. This value is based on the average global horizontal irradiance (GHI) given by TMY3 data for Terre Haute, Indiana on a typical summer day. The ratio of average GHI to the net extraterrestrial global radiation yields a typical solar influence factor. In this case, 30% was found to realistically represent the region. Reflected solar radiation is ignored in this analysis. Reflected radiation from a still water surface at an incidence directly normal to the surface was assumed to be 4%. This value would be significantly smaller for a disturbed surface as found in a flowing canal; thus reflected radiation is ignored in this analysis.

The cooling canals can reject the required 1.16GW with 25 canals, each canal of 10 m width, 0.3 m depth, and 9.6 km length for a total footprint area of 2,400,000 m^2. The temperature of the condenser discharge water is 45 °C, and the mass flow rate is 1143 kg/s.

2.2. Open-Water Algae Bioreactor Pond:

The open-water algae bioreactor is a pond assumed to be circular in shape. The algae bioreactor pond is treated as being opaque and well-mixed. The reflectivity of solar radiation is assumed to be 4% [15]. As in the case of the cooling canal, the bottom of the algae bioreactor pond is considered insulated. The heat rejected from the algae bioreactor pond is a function of the water temperature and the environmental conditions. It is assumed that the algae bioreactor pond is subject to an ambient wind. A representation of the energy exchange in the algae bioreactor pond is provided in Figure 2.

Although the solar insolation has a negative effect on heat loss from the algae bioreactor pond, the sun helps the growth of algae which require light for the photosynthetic process. The energy balance on the algae bioreactor pond involves heat input provided from the power plant discharge, the absorbed solar heat input, and the enthalpy of the makeup water to replace the mass evaporated. The energy lost from the algae bioreactor pond consists of emitted and reflected radiation components, combined heat and mass transfer to the ambient, and solar energy absorbed by the algae. The energy balance can be represented as:

$$\dot{Q}_{plant} + \dot{Q}_{solar} + \dot{m}_{makeup}\mathbf{h}_{makeup} = \dot{Q}_{em} + \dot{Q}_{refl} + \dot{Q}_{hm} + \dot{Q}_{algae} \tag{7}$$

$$\dot{Q}_{solar} = A\alpha_{solar}G_{rad} \tag{8}$$

$$\dot{Q}_{em} = A\varepsilon\sigma\left(T_s^4 - T_\infty^4\right) \tag{9}$$

$$\dot{Q}_{refl} = A\rho G_{rad} \tag{10}$$

$$\dot{Q}_{algae} = A\alpha_{photo}G_{rad} \tag{11}$$

$$\dot{Q}_{hm} = \left(\bar{h}/c_{p,vapor}\right)A(\mathbf{h}_s - \mathbf{h}_\infty) \tag{12}$$

where the convection coefficient is given by Pohlhausen [16] as,

$$\bar{h} = \left({}^{k_{air}}\!\!\diagup\!\!{}_{L} \right)\left(0.037 Re^{4/5} - 871\right) Pr^{1/3} \tag{13}$$

and α_{photo} is assumed to be 7% [17]. For a thermophilic algae bioreactor pond, the algae production rate (ζ_{algae}) is assumed to be 12 grams of algae per square meter per day, the average caloric value of algae (λ_{algae}) to be 36 kJ/g, and the mass percentage of oil in the algae (ξ_{algae}) to be 36% [17]. This translates into 155.52 kJ/m^2/day as given by the calculation of the chemical potential of the algae bioreactor pond:

$$\dot{E}''_{algae} = \zeta_{algae} \lambda_{algae} \xi_{algae} \tag{14}$$

While this estimate is used in the present work as the more conservative value, Sheehan *et al*. [18] suggested a higher algae production rate of up to 50 grams of algae per square meter per day (yielding an energy production rate of 648 kJ/m^2/day).

Using the above production rate calculated from Benemann *et al.* [17], an algae bioreactor pond that is 538,232 m^2 in area with makeup water temperature (T_{makeup}) of 45 °C, can reject 1.16 GW of heat discharged from a power plant as well as 220.8 MW of solar radiation. The pond surface temperature is calculated to be 62 °C which can potentially produce 969.2 kW of energy from the algae biomass.

2.3. Wintertime Greenhouse Heating:

Heat is conducted to a greenhouse by running condenser discharge water through pipes beneath the soil. Radiation from the soil to the ambient is considered negligible as the greenhouse enclosure is designed to allow the passage of incident radiation but not that of emitted radiant heat from inside the greenhouse. The soil is assumed to be dry with the plants having minimal impact; therefore, evapotranspiration is ignored. As in Chou *et al.* [7], the air in the greenhouse is considered well-mixed. The greenhouse is assumed to be housed under a double-glazed transparent plastic enclosure. The analysis assumes that the heat transfer is one-dimensional and under steady conditions. Heat is transferred from the hot water to the pipes through convection. It is then conducted through the soil, the air in the greenhouse, and the double glazed transparent plastic, before being released to the atmosphere via convection. As in the previous two analyses, the ground is considered insulated. Under steady-state conditions, to the ground represents a significantly higher thermal resistance compared with the path to ambient [18]. As heat is transferred to ambient air through each part of the greenhouse, it encounters a series of thermal resistances, as represented by the network in Figure 3. This thermal resistance network is used to determine the steady-state heat transfer in the greenhouse, as indicated in the equations below, as follows:

$$R''_{total} = \frac{1}{h_{water}} + \frac{l_{pipe}}{k_{pipe}} + \frac{l_{soil}}{k_{soil}} + \frac{1}{h_{green}} + \frac{l_{plastic}}{k_{plastic}} + \frac{l_{air}}{k_{air}} + \frac{l_{plastic}}{k_{plastic}} + \frac{1}{h_{amb}} \tag{15}$$

where,

$$h_{water} = \frac{k_{water} 0.023 Re_D^{4/5} Pr^{2/5}}{D} \tag{16}$$

$$h_{green} = \frac{k\left(0.664 Re^{1/2} Pr^{1/3}\right)}{L} \tag{17}$$

$$h_{amb} = \frac{k\left(0.037 Re^{4/5} - 871\right) Pr^{1/3}}{L} \tag{18}$$

The convection coefficient in equation (16) is from Winterton [20], while the convection coefficients in equations (17) and (18) are due to Pohlhausen [16]. Finally the combined heat flux leaving the greenhouse can be written as:

$$Q'' = R''_{total}(T_{\infty,water} - T_{\infty,amb}) \tag{19}$$

The heat rejected is thus a function of the pipe depth, pipe spacing, greenhouse width, and greenhouse length. The required heat load of 1.16GW can be rejected from the plant assuming the pipes in the soil are 0.5 m apart and placed 0.25 m beneath the soil; each greenhouse is assumed to be 100 m long and 100 m wide with an inlet water temperature of 45 °C. A total of 530 such greenhouse units are required with a total greenhouse footprint of 5,300,000 m^2.

2.4. Spray Pond:

A typical spray pond consists of an array of nozzles in groups of four or five that spray condenser discharge water into the ambient air; the discharge water is then collected into the pond. The present analysis calculates the heat transfer from a single nozzle, treated independently, and free from the effects of wind and interaction with sprays from surrounding nozzles. The spray heat transfer calculated here assumes that the nozzle is positioned at the surface of the pond and the spray issues upward. The heat transfer from the spray is calculated from the droplet average velocity, the droplet residence time, and the Sauter mean diameter of the droplets [8] defined as

$$D = 6\left(V_{drop} / A_{drop}\right) \tag{20}$$

The evaporative heat transfer is calculated from the heat and mass transfer analogy. The mass evaporated from the droplets is of the order of 1% [21]; therefore, a constant droplet diameter is assumed.

The heat transfer coefficient between the droplet and ambient air is given by Whitaker [22] as:

$$h = {k_{air}}/{D}\left[2 + \left(0.4 Re_D^{1/2} + 0.06 Re_D^{2/3} \right) Pr^{2/5} \right] \quad (21)$$

Then, the steady state convective and evaporative heat transfer is calculated assuming an average droplet temperature:

$$\dot{Q}_{conv} = hA_{drop}\left(T_{avg} - T_{\infty,amb} \right) \quad (22)$$

$$\dot{Q}_{evap} = h_{hm}\left(\rho_s - \varphi \rho_\infty \right) A_{drop} h_{fg} \quad (23)$$

where the density of the water vapor at the surface of the drop is evaluated at the average droplet temperature. Since the average droplet temperature is unknown, an energy balance must be enforced as follows:

$$\dot{Q}_{conv} + \dot{Q}_{evap} = \dot{m}_{w,in} h_{w,in} - (\dot{m}_{w,out} - \dot{m}_{w,evap}) h_{w,out} \quad (23)$$

The selected heat rejection requirement of the plant can be met if 14,630 nozzles are used over a 365,750 m^2 pond. The mass flow rate of each nozzle is 1.8 kg/s with an average droplet size of 2 mm. The initial and final temperatures of the condenser discharge water are 45 °C and 35 °C, respectively.

2.5. Modified Solar Updraft Tower:

The air flow in the modified solar updraft tower is used to remove heat from the condenser discharge water of the power plant using a secondary fluid circuit. The difference in working fluid between the solar updraft tower and the technologies considered thus far disallows the same fluid temperature being used as a basis for comparison. Therefore, the solar updraft down will instead be required to reject 1.16 GW of heat using this second fluid, which will match the heat rejection of the 500 MW plant. This circuit carries refrigerant between the condenser and a plate fin heat exchanger at the perimeter of the solar collector. The induced air draft is used to extract work from the air stream by means of a turbine at the base of the tower.

A staggered-tube plate fin heat exchanger was selected with a prescribed geometry as shown in Figure 5. The heat exchanger is placed at the outer radius of the solar updraft tower to maximize heat transfer effectiveness between the working fluid and the ambient air. The heat exchanger design was selected for its low pressure drop characteristics. The heat exchanger span in the air flow direction is small relative to the collector diameter; therefore, the decrease in the heat exchange loop radii from the entrance to the exit of the heat exchanger is neglected. This allows for the assumption of a constant cross-sectional area from the heat exchanger inlet to outlet. The height of the heat exchanger is 3.5 m, and the length of the heat exchanger in the air flow direction is 10 m. Schematic drawings of the modified solar updraft tower and heat exchanger geometry can be seen in Figure 4 and Figure 5, respectively.

The pressure drop in the tower is calculated using Bernoulli's equation [23]. The following expressions relate the various pressures, and are used to calculate the velocity and mass flow rate in the tower:

$$P_1 = P_0 - \frac{\rho_0 U_1^{\,2}}{2} \tag{24}$$

$$P_4 = P_0 - \rho_0 g z_{tower} \tag{25}$$

$$P_4 = P_3 - \frac{\rho_3 \left(U_4^{\,2} - U_3^{\,2} \right)}{2} - \rho_3 g \left(z_{tower} - z_{collector} \right) \tag{26}$$

$$P_1 - P_2 = \frac{\mathbf{G}_{max}^2 v_1}{2} \left[\left(1 + \boldsymbol{\sigma}^2 \right) \left(v_2 / v_1 - 1 \right) + f \left(A_s / A_{ff} \right) \frac{\left(v_1 + v_2 \right)}{2 v_1} \right] \tag{27}$$

where $\mathbf{G}_{max}$ is the maximum mass velocity such that,

$$\mathbf{G}_{max} = \rho V_{max} \tag{28}$$

Ambient air at point 0 moves toward the inlet of the plate fin heat exchanger at point 1. The air passes through the heat exchanger, entering the area under the collector at point 2 where it is heated by solar radiation before it enters the tower at point 3 and is exhausted to the atmosphere at point 4. Each of these state points is depicted in Figure 4. The heat exchanger pressure drop is calculated as recommended by Kays and London [24].

The heat transfer in the heat exchanger was analyzed using the ε-NTU method. The convective heat transfer coefficient for the secondary fluid inside the tubes is given by Chato [25]:

$$\bar{h}_D = 0.555 \left[\frac{g \rho_l \left(\rho_l - \rho_{vapor} \right) k_l^3 h_{fg}^{'}}{\mu_l \left(T_{sat} - T_s \right) D} \right] \tag{29}$$

The air side convective heat transfer coefficient is calculated from the Nusselt number given by Kays and London [24] as:

$$h = \frac{0.011 k}{D_{hyd}} \left[\mathbf{G}_{max} c_{p,air} \frac{D_{hyd} Re_D^{\,-0.418}}{k_2 Pr^{2/3}} \right] \tag{30}$$

The overall UA value can then be calculated and the ε-NTU analysis conducted using:

$$UA \cong \frac{1}{\frac{1}{\eta_{fin}\bar{h}_D A_{tubes}} + \frac{1}{hA_s}} \tag{31}$$

$$NTU = \frac{UA}{\dot{m}_{air} c_{p,air}} \tag{32}$$

$$\varepsilon = 1 - exp(-NTU) \tag{33}$$

Finally, the heat rejected from the plant to the air in the tower can be represented by:

$$\dot{Q}_{plant} = \varepsilon \dot{m}_{air} c_{p,air} \left(T_{f,i} - T_1 \right) \tag{34}$$

The heat gain in the collector accounts for solar gains and external convective losses. The collector heat gain is given by Schlaich [26]:

$$\dot{Q}_{collector} = \left(\alpha G_{rad} - \beta \Delta T_{collector} \right) A \tag{35}$$

The available power from the updraft is given by Padki and Sherif [11]:

$$\dot{W} = \frac{\sqrt{2\left(g z_{tower} \Delta T_{1,3} \right)^3 / T_0} \rho_0 A_{tower}}{\left(T_0 + \Delta T_{1,3} \right)} \tag{36}$$

The slope of the collector from the inlet to the base of the tower is set as a constant 1 cm/m to be consistent with the analysis of Schlaich [26]. The tower diameter is set to 102.5 m, and the tower height to 850 m. The collector diameter is 2500 m for a total footprint area of 4,900,000 m^2. The heat exchanger height and depth are 3.5 m and 10 m, respectively. A modified solar updraft tower with this geometry can reject the required 1.16 GW of heat load through the heat exchanger as well as absorb 3.44 GW of solar energy and produce 99.27 MW of power. This corresponds to first and second law thermodynamic efficiencies of 2.1% and 33.3%, respectively.

3. Discussion of Results

Each of the heat-rejection technologies considered in this work has been shown above to be capable of rejecting the required amount of waste heat. This section explores the benefits and shortcomings of these approaches. Each technology is compared for the land use required, the limitations regarding ambient conditions under which the design performance is achieved, and the sensitivity of the system to the different geometric and environmental parameters.

3.1. Footprint Comparison

The area (land use) required to accomplish the required heat rejection is the most critical parameter in the design of the cooling canals, open-water algae bioreactor ponds, and spray ponds. The large

surface area of the condenser discharge water in the spray ponds allows for more efficient use of land area compared to cooling canals and open-water algae bioreactors.

Although the algae bioreactor pond and cooling canals reject heat through the same pathways, the cooling canals require more surface area because the algae bioreactor pond operates at a higher average temperature. The greenhouse heating and the modified solar updraft tower occupy the greatest land area, but offer other salutary effects such as allowing for crop production in winter, or power production using a turbine, respectively.

3.2. Limitations from Ambient Conditions

The greenhouse heating option would not be a viable alternative in hot weather and can only be used in the wintertime in northern climates. The portion of the year when greenhouse heating is effective is shown in Figure 6 while Figure 7 shows the days of the year during which the greenhouse would need to be cooled. The climate conditions in this study are from TMY3 data from Hulman Regional Airport in Terre Haute, Indiana (1994-2005). The other four alternative heat rejection approaches investigated also experience significant degradation in performance during hot, humid ambient conditions but would continue to reject heat as long as there is a favorable temperature difference between the condenser discharge temperature and the ambient. Higher wind speeds also give rise to enhanced heat transfer for each case; however, high wind speeds may decrease the power output of the modified solar updraft tower due to greater convective losses from the solar collector. In extremely cold climates, the spray pond, cooling canals, and algae pond may not function unless they are prevented from freezing.

Solar radiation has a significant impact on the performance of the algae bioreactor pond, greenhouse heating and solar updraft tower. The solar radiation assists in the operation of the solar updraft tower. The solar radiation aids in heating the greenhouse, but takes away from the amount of power plant discharge heat that can be rejected. The absence of solar radiation degrades the performance of the solar updraft tower, whereas, the performance of the heat rejection to the greenhouse and algae improves with lower levels of solar radiation. The algae bioreactor pond, cooling canals, and spray ponds are also negatively affected by increased solar radiation.

3.3. System Sensitivity

The analytical models developed here allow for the sensitivity of the performance of the cooling canals, algae bioreactor pond, spray pond, and modified solar updraft tower to ambient conditions, condenser discharge water temperatures, and geometric parameters to be determined. A sensitivity study of the greenhouse heating option was not explicitly conducted as the seasonal limitations restrict its use as outlined in Figure 6 and Figure 7. For each approach, the parameters that influence the system requirements and performance the most were varied within typical operating and geometric ranges.

Heat rejection from the cooling canal is governed by the available surface area, condenser discharge temperature, and environmental conditions including average wind speed. Figure 8 shows the cooling

canal heat transfer as a function of the ambient temperature for various wind speeds, assuming a fixed canal surface area where each of the 25 canals is 9.6 km long and 10 m wide. The heat transfer increases with decreasing ambient temperature, due to the increasing temperature differential available. The canal heat transfer also increases with ambient wind speed due to the enhanced convective heat transfer. Figure 9 shows the surface temperature of the pond as a function of the area of the pond for various ambient wind speeds with a fixed heat rejection rate of 1.16 GW. The temperature of the algae pond is influenced by the surface area of the pond, the ambient wind speed, and the ambient temperature. The relationship between pond area and ambient wind speed is explored because these parameters have the greatest effect on the pond temperature. For a fixed heat load, the surface temperature of the pond increases as the size of the pond decreases, or as the ambient temperature increases. The pond surface temperature decreases as the ambient wind speed increases. The operating temperature of the algae bioreactor pond is constrained by the range of temperatures required for algal growth with an upper limit of algae growth of about 75 °C [17]. An operating temperature that is too low reduces algae yields and requires a large pond. An operating temperature that is too high similarly affects algae yield adversely.

Heat rejection from the spray pond is shown in Figure 10 as a function of the condenser discharge temperature for different droplet diameters, at a fixed mass flow rate. The spray pond performance is sensitive to the type of spray nozzle used. The spray trajectory is an important determinant of the heat rejected because it dictates the average velocity and residence time of each droplet. Ambient temperature and relative humidity are also very important to the calculated heat transfer rates. As the ambient temperature falls or the condenser discharge temperature increases, more heat is rejected from the spray. High ambient relative humidity, on the other hand, degrades the evaporative heat transfer from the spray. For a given mass flow rate, a smaller droplet diameter leads to a greater surface area, and hence, to improved performance.

Figure 11 presents the heat rejection and power production of the modified solar updraft tower as functions of the ambient temperature, for fixed tower dimensions. The performance of the modified solar updraft tower is sensitive to a number of parameters including tower height, tower diameter, and collector diameter. The heat transfer, power production, and mass flow rate of air increase as ambient temperature decreases. For a fixed heat exchanger geometry, a change in the collector diameter directly impacts the heat exchanger area and thus the amount of heat rejected from the plant.

3.4 Net System Water Use

The net water lost to the environment with the different technologies considered is compared here. Both the modified solar updraft tower as well as the greenhouses incur no net water loss to the environment due to evaporation. This is because both of these solutions are ‘closed,’ and do not rely on evaporative heat transfer to reject heat. However, the algae bioreactor, spray cooling pond, and cooling canals are predicted to evaporate water at a rate of 334, 415, and 539 kg/sec, respectively; this compares to 442 kg/sec for a typical cooling tower [13]. The evaporation rate decreases with an increase in operating temperature of the technology. The algae bioreactor operates at a significantly higher temperature than the spray pond or cooling canals. This allows the sensible heat transfer to

increase, and also for the overall area required to be reduced. Since the relative humidity is fixed for all comparisons, the increased temperature and reduced footprint area combine to result in an overall reduction in evaporative water loss.

4. Conclusions

Five alternative options for the rejection of large amounts of condenser discharge heat from power plants are analyzed and discussed. The options include cooling canals, open-water algae bioreactor ponds, greenhouse heating, spray ponds, and modified solar updraft towers. The following conclusions can be drawn based on the analysis.

The modified solar updraft tower, cooling canal, algae bioreactor pond, and greenhouse each require a large land area. However, modified solar updraft towers, algae bioreactors, and greenhouse heating each provide a useful secondary output. Additionally, greenhouse heating is only viable in the winter months or in extreme northern climates, and the solar updraft tower may not perform well in an area with little solar insolation. The algae bioreactor pond can be used to recycle carbon dioxide from flue gases as well as reject heat from the plant and produce biomass. However, the temperature of the algae bioreactor must be closely monitored for the health of the algae. The spray pond is a good option if land resources are limited and supply of the required pumping power is not a serious concern.

The net water use of four of the five options was found to be less than that of the baseline technology, the cooling tower. This has significant implications on overall environmental impact and operating cost of the cooling solution. The cooling canals incur significantly more water use than a cooling tower, but with much less complexity.

This study considered only the climate conditions representative of the Midwestern United States. The climate conditions will likely have a significant impact on the overall performance of each potential solution presented. Therefore, careful consideration of the climate is recommended, particularly with respect to water use. The net water use would become more significant in a more arid region.

Some of these options, such as cooling canals and spray ponds, could be used in combination to increase the heat transfer performance. These technologies can be used as viable alternatives to cooling towers, and at the same time, do not present the same threat to the environment as heat rejection to lakes and streams with similar or less water use. Further development and optimization of the options analyzed here could significantly benefit the cause of mitigating global climate change and improving power plant overall efficiencies.

5. Nomenclature

A	area [m^2]
A_{surf}	total air side heat transfer surface area of heat exchanger [m^2]
A_{ff}	minimum free flow area of the finned passages perpendicular to the flow direction in heat exchanger [m^2]
c_p	specific heat [kJ kg^{-1} K^{-1}]
$\overline{D}$	average diameter [m]
D	diameter [m]
$\dot{E}$"	energy flux [kJ m^{-2} day^{-1}]
f	friction factor in the heat exchanger [-]
g	gravitational constant [m s^{-2}]
$\mathbf{G}_{max}$	maximum mass velocity [kg m^{-2} s^{-1}]
G_{rad}	irradiation [Wm^{-2}]
h	convective heat transfer coefficient [W m^{-2} K^{-1}]
h	enthalpy [kJ kg^{-1}]
h_{fg}	heat of vaporization [kJ kg^{-1}]
h_m	mass transfer coefficient [m s^{-1}]
k	thermal conductivity [W m^{-1} K^{-1}]
L	length [m]
Le	Lewis Number [-]
$\dot{m}$	mass flow rate [kg s^{-1}]
Nu	Nusselt Number [-]
NTU	Number of Transfer Units [-]
P	pressure [kPa]
Pr	Prandtl Number [-]

$\dot{Q}$	heat transfer rate [W]
Re	Reynolds Number [-]
T	temperature [°C]
t	time [s]
U	velocity [m s^{-1}]
v	specific volume [m^3]
V	volume [m^3]
$\dot{V}$	volumetric flow rate [m^3 s^{-1}]
$\dot{W}$	power [kW]
Z	height [m]

Greek

α	absorptivity [-]
β	convective loss coefficient [W m^{-2} K^{-1}]
Δ	change [-]
ε	emissivity [-]
ζ	algae production rate [kg m^{-2} day^{-1}]
Θ	angle [deg]
λ	caloric value of algae [kJ kg-1]
μ	dynamic viscosity [N s m^{-2}]
ξ	mass percentage of algae oil [-]
ρ	density [kg m^{-3}]
σ	Stefan-Boltzmann constant [W m^{-2} K^{-4}]
$\boldsymbol{\sigma}$	ratio of the minimum free flow area of the finned passages perpendicular to the flow direction (A_{ff}) to the frontal flow area of the heat exchanger in heat exchanger [-]
ϕ	relative humidity [-]

Subscripts

abs	absorbed
amb	ambient
avg	average
conv	convection
crit	critical
D	larger diameter
d	smaller diameter
em	emitted
evap	evaporation
f	final
fg	fluid to gas vaporization
fin	heat exchanger fin
hm	combined heat and mass transfer
hyd	hydraulic
i	initial
∞	free stream property
l	liquid
L	length
photo	photosynthesis
rad	radiation
refl	reflected
s	surface
sat	saturation

Acknowledgement

The authors acknowledge useful technical discussions and support for this work from Hoosier Energy Rural Electric Cooperative, a Touchstone Energy Cooperative serving Indiana.

6. References

[1] Frediani HA. Cooling canal system modeling report. Atlanta (GA): Golder Associates Inc.; 2008 Jan. Report No. 1670.

[2] Demirbas MF. Biofuels from algae for sustainable development. Applied Energy 2011;88:3473-3480.

[3] Chisti Y, Yan J. Energy from algae: Current status and future trends. Applied Energy 2011;88, 3277-3279.

[4] Ryan PJ, Harleman DR, Stolzenbach KD. Surface heat loss from cooling ponds. Water Resour Res 1974;10:930-8.

[5] Chinese D, Meneghetti A, Nardin G. Waste-to-energy based greenhouse heating: exploring viability conditions through optimisation models. Renew Energy 2005;30:1573-86.

[6] Manning TO, Mears DR. Engineering performance of a 1.1 hectare waste-heated greenhouse. Proceedings from the Summer Meeting of the American Society of Agricultural Engineers; 1983 Jun 26-29; Bozeman, MT.

[7] Chou SK, Chua KJ, Ho JC, Ooi CL. On the study of an energy-efficienc greenhouse for heating, cooling and dehumidification applications. Applied Energy 2004; 77,355-373.

[8] Chen KH, Trezek GJ, editors. Spray energy release approach to analyzing spray system performance. Proceedings of the American Power Conference; 1976;38:1435-48.

[9] Porter RW, Chaturvedi SK. Unit thermal performanceof atmospheric spray cooling systems. J Heat Transf 1980;102:210-4.

[10] Codell RB. Performance model for ultimate heat spray ponds. J Energy Eng 1986;112:71-89.

[11] Padki MM, Sherif SA. On a simple analytical model for solar chimneys. Int J Energy Res 1999;23:345-9.

[12] Nizetic S, Klarin, B. A simplified analytical approach for evaluation of the optimal ratio of pressure drop across the turbine in solar chimney power plants. Applied Energy 2010;87,587-591.

[13] Feeley TJ, Green L, Murphy JT, Hoddmann J, Carney BA. Department of Energy/Office of Fossil Energy's Power Plant Water Management R&D Program. US Department of Energy. July 2005.

[14] Churchill SW, Ozoe H. Correlations for laminar forced convection with uniform heating in flow over a plate and in developing and fully developed flow in a tube. J Heat Transf 1973;95C:78-84.

[15] Ryan PJ, Harleman DRF, Stolzenbach KD. Surface heat loss from cooling ponds. Water Resources Research. 1974; 10 No. 5: 930-938.

[16] Pohlhausen E. Der wärmeaustausch zwischen festen körpern und flüssigkeiten mit kleiner reibung und kleiner wärmeleitung. Z Angew Math Mech 1921;1:115-21. German.

[17] Benemann JR, Weissman JC, Koopman BL, Oswald WJ. Energy production by microbial photosynthesis. Nature 1977;268:19-23.

[18] Sheehan J, Dunahay T, Benemann J, Roessler P. A look back at the US department of energy's aquatic species program---biodiesel from algae. Final Report. Golden (CO): National Renewable Energy Laboratory; 1998 Jul. Report No.: NREL/TP-580-24190. Contract No.: DE-AC36-83CH10093.

[19] Freemyers MC. Waste Heat Utilization for Greenhouse Climate Control [thesis]. West Lafayette (IN). Purdue University; 1977.

[20] Winterton RH. Where did the Dittus and Boelter equation come from? Int J Heat Mass Transf 1998;41:809-10.

[21] Moussiopoulos N. Numerical simulation of spray cooling pond performance. J Fluids Eng 1987;109:179-85.

[22] Whitaker S. Forced convection heat transfer correlations for flow in pipes, past flat plates, single spheres, and for flow in packed beds and tube bundles. Am Inst Chem Eng J 1972;18:361-71.

[23] Fisher TS, Torrance KE, Sikka KK. Analysis and optimization of a natural draft heat sink system. IEEE Trans Compon Packag Technol 1997;20:111-9.

[24] Kays WM, London AL. Compact Heat Exchangers. 3rd ed. New York: McGraw-Hill; 1984.

[25] Chato JC. Laminar condensation inside horizontal and inclined tubes. ASHRAE J 1962;4:52-60.

[26] Schlaich J. The Solar Chimney: Electricity from the Sun. (M. Robinson, Trans.) Stuttgart: Edition Axel Menges; 1995.

Figure Captions

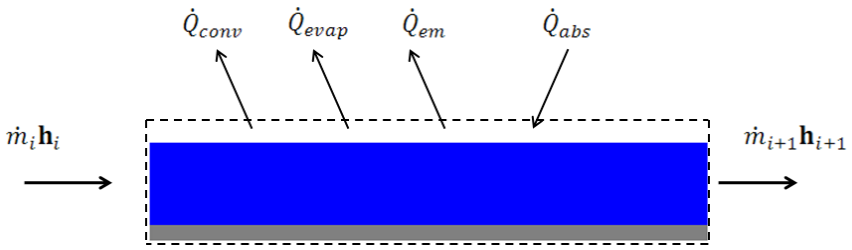

Figure 1. Control volume for one canal segment.

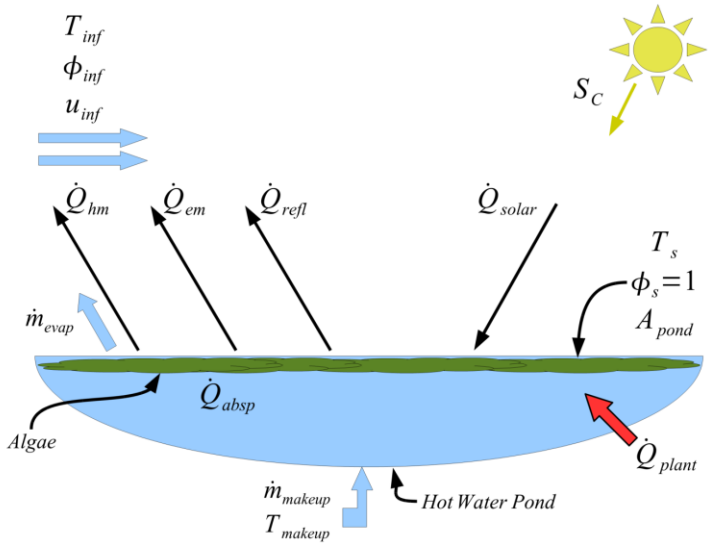

Figure 2. Algae bioreactor pond control volume.

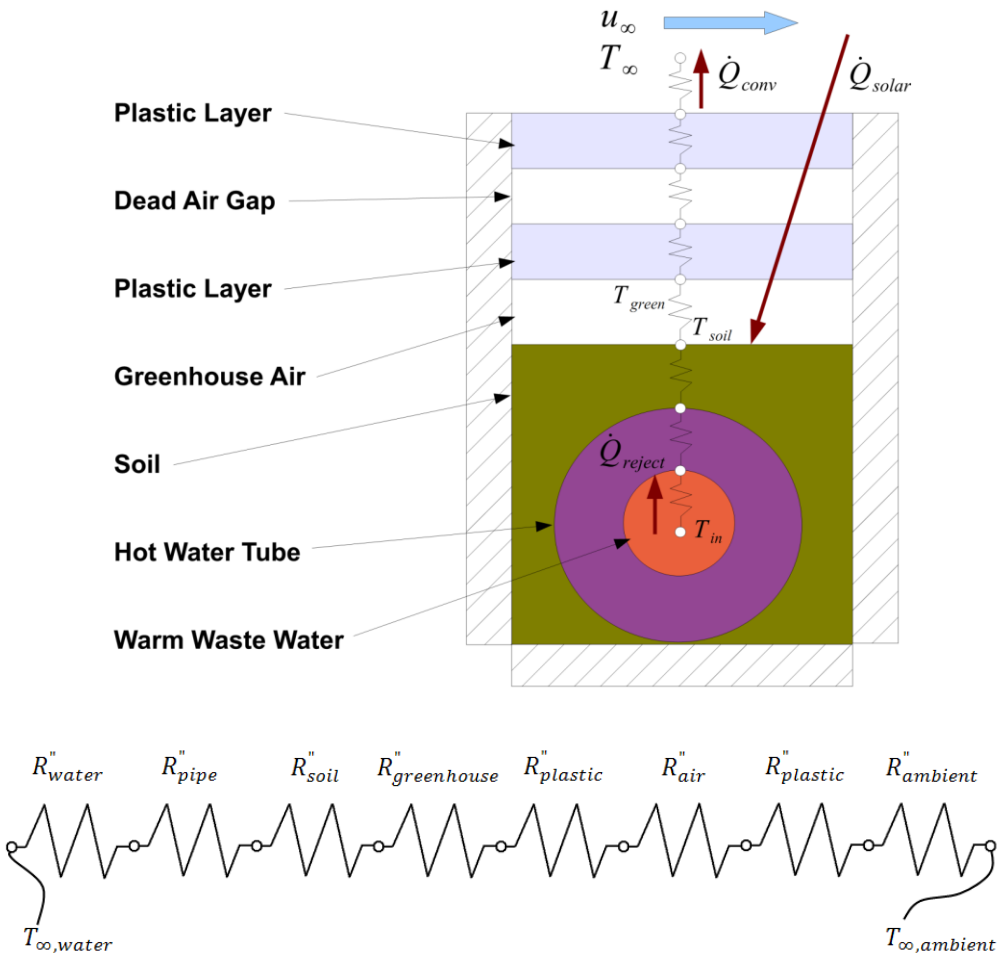

Figure 3. Greenhouse thermal resistance network.

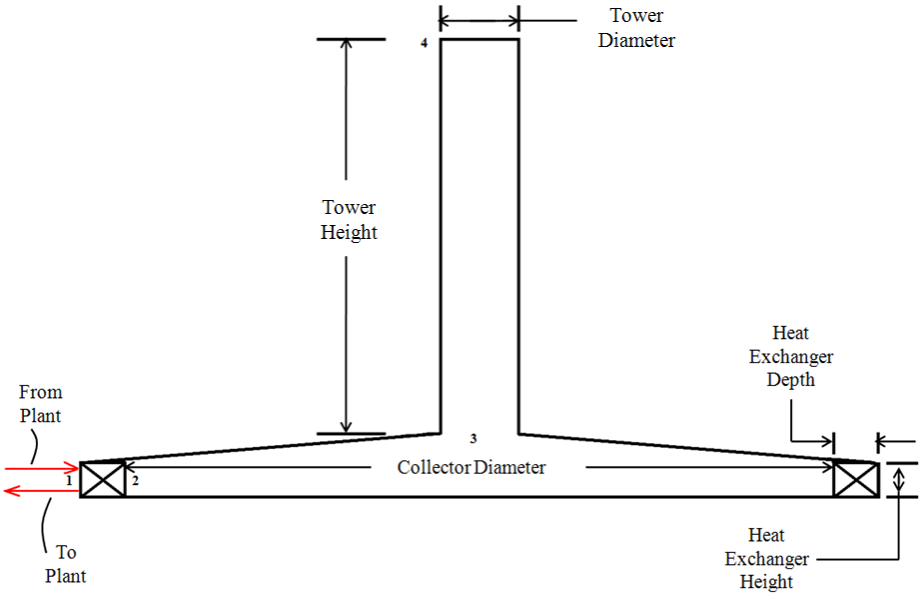

Figure 4. Modified solar tower schematic figure.

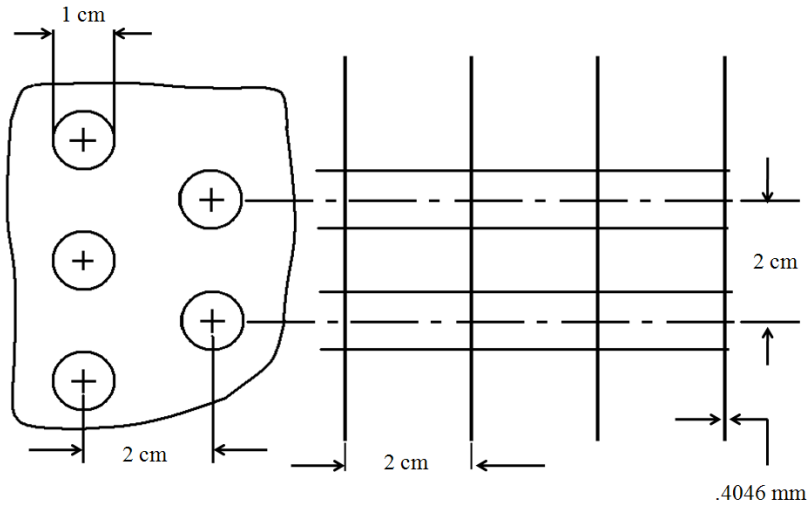

Figure 5. Heat exchanger geometry in a modified solar tower.

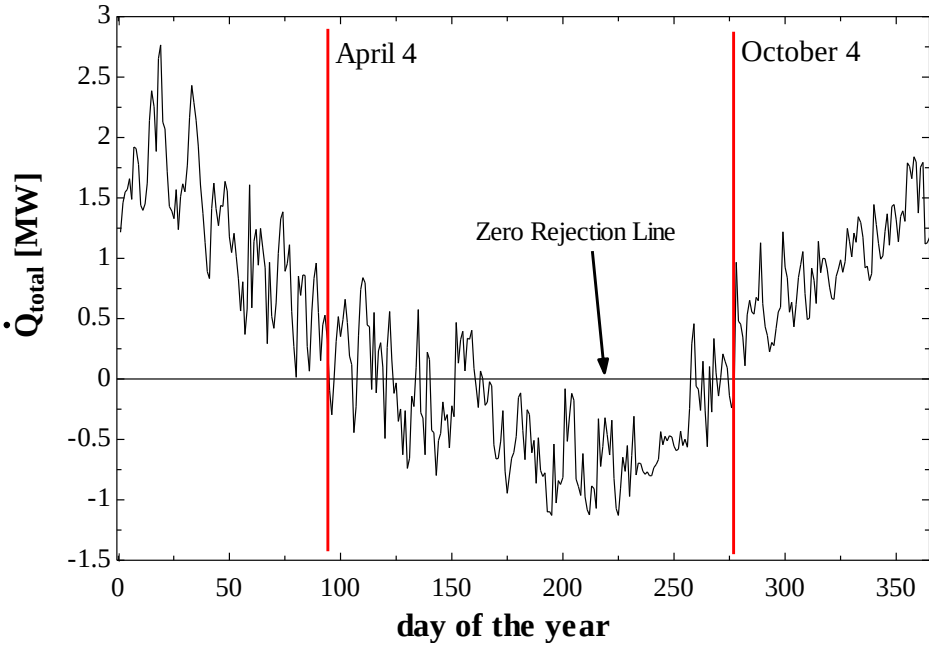

Figure 6. Timetable for effective use of greenhouse heating from the Hulman Regional Airport in Terre Haute, Indiana (1994-2005).

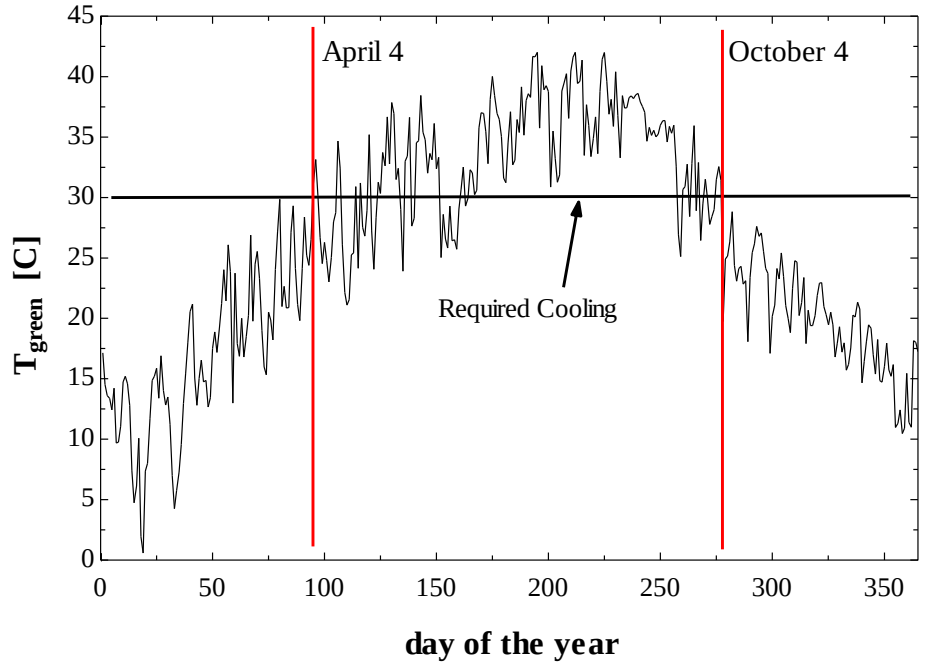

Figure 7. Timetable for required greenhouse cooling from the Hulman Regional Airport in Terre Haute, Indiana (1994-2005).

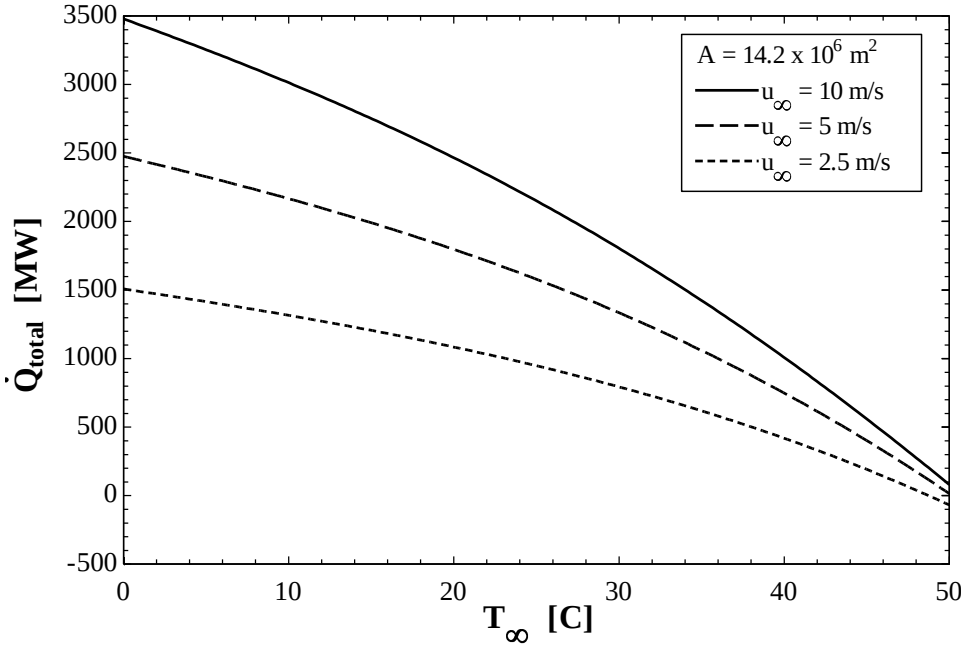

Figure 8. Total canal heat transfer versus ambient temperature for various wind speeds.

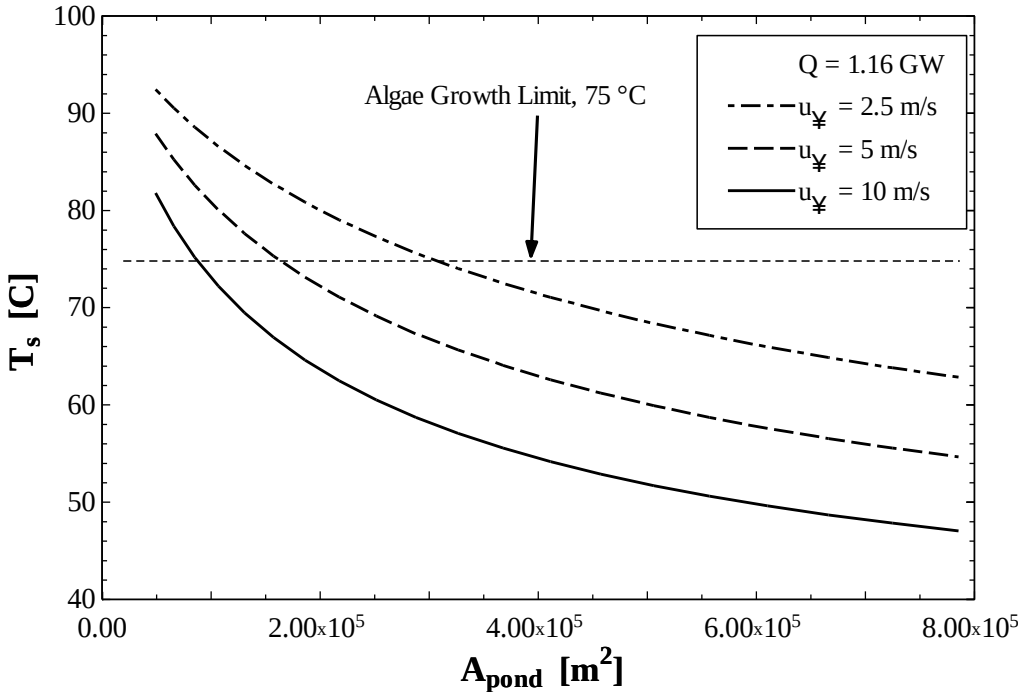

Figure 9. Algae bioreactor pond temperature versus pond area for various wind speeds.

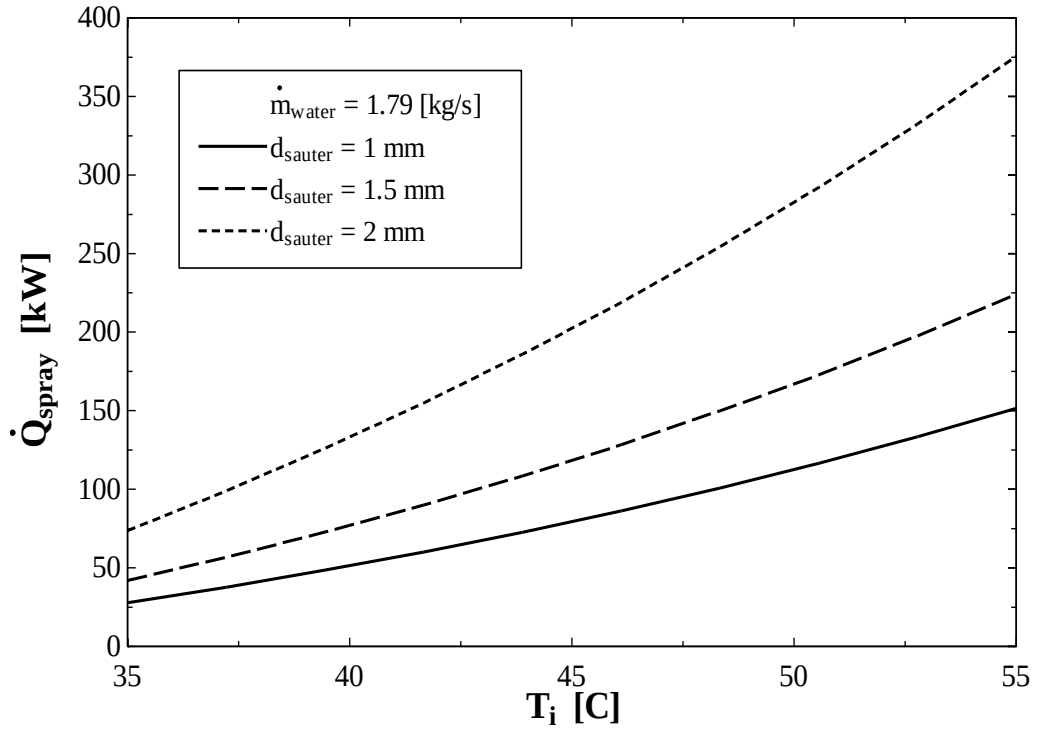

Figure 10. Spray heat transfer for a single nozzle versus condenser discharge temperature for various droplet diameters.

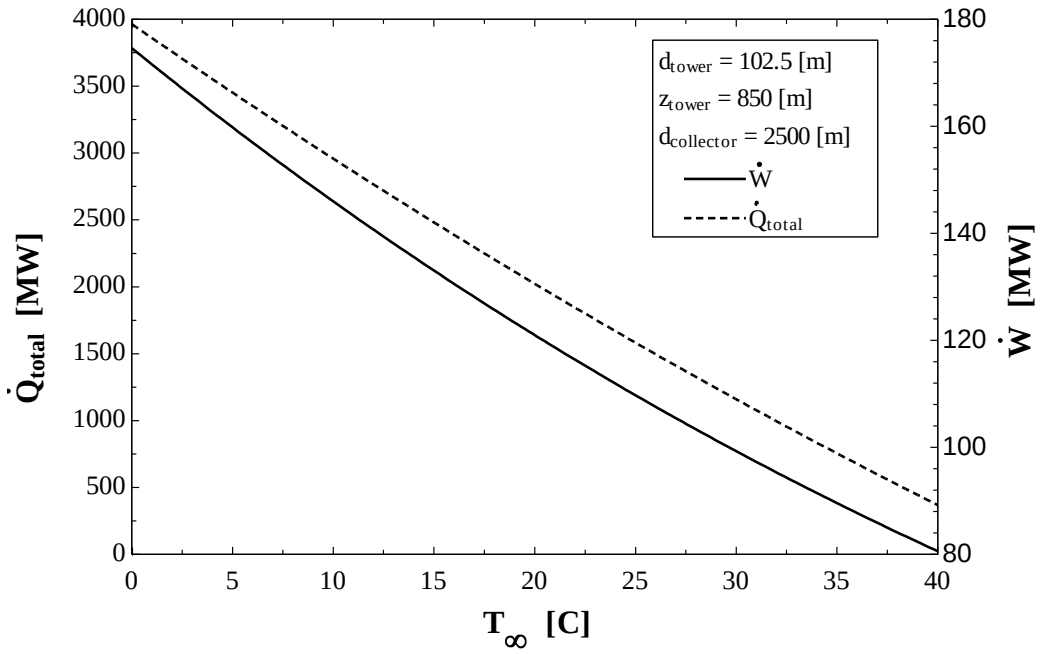

Figure 11. Modified solar tower heat rejection and power production versus ambient temperature.